January 1, 2008

Wide varieties of cationic nanoparticles induce defects in supported lipid bilayers

PR Leroueil
SA Berry
K Duthie
G Han
VM Rotello, et al.

NANO LETTERS

2008
Vol. 8, No. 2
420−424

Wide Varieties of Cationic Nanoparticles Induce Defects in Supported Lipid Bilayers

Pascale R. Leroueil,[†,||] Stephanie A. Berry,[‡,||] Kristen Duthie,[†,||,‡] Gang Han,[⊥] Vincent M. Rotello,[⊥] Daniel Q. McNerny,[§,||] James R. Baker, Jr.,[||] Bradford G. Orr,[‡,||] and Mark M. Banaszak Holl*[,†,||]

Departments of Chemistry, Physics, Chemical Engineering, Michigan Nanotechnology Institute for Medicine and Biological Sciences, University of Michigan, Ann Arbor, Michigan 48019, and Department of Chemistry, University of Massachusetts, Amherst, Massachusetts 01003

Received September 7, 2007; Revised Manuscript Received December 20, 2007

ABSTRACT

Nanoparticles with widely varying physical properties and origins (spherical versus irregular, synthetic versus biological, organic versus inorganic, flexible versus rigid, small versus large) have been previously noted to translocate across the cell plasma membrane. We have employed atomic force microscopy to determine if the physical disruption of lipid membranes, formation of holes and/or thinned regions, is a common mechanism of interaction between these nanoparticles and lipids. It was found that a wide variety of nanoparticles, including a cell penetrating pepide (MSI-78), a protein (TAT), polycationic polymers (PAMAM dendrimers, pentanol-core PAMAM dendrons, polyethyleneimine, and diethylaminoethyl-dextran), and two inorganic particles (Au-NH_2, SiO_2-NH_2), can induce disruption, including the formation of holes, membrane thinning, and/or membrane erosion, in supported lipid bilayers.

Nanoparticles are currently employed or proposed for a variety of products including drug and gene delivery materials,[1,2] industrial applications such as catalysts,[3] and consumer products including paints[4] and lotions.[5] Although the technical benefits of using nanoparticles for each particular implementation are clear, the broader impacts of the release of such materials into the environment have yet to be understood.[6−8] One concern is the cytotoxicity of these materials. An interaction of particular interest is that between the cell plasma membrane and nanoparticles, as this is the basic structure of the cell that may be breached with concomitant cytotoxicity.

A great deal of empirical evidence suggests that nanoparticles are effective disruptors of cell plasma membranes. Ready access to this work is provided by a number of recently published papers demonstrating both in vitro,[9−13] as well as in vivo[13−18] nanoparticle activity with membranes. Specifically, cell level data have demonstrated evidence for membrane permeability via enzyme leakage assays[7,10,12,19] and dye diffusion studies.[12] Direct evidence that the nanoparticles disrupt lipid bilayers was provided by electron paramagnetic resonance.[20,21] Studies on supported lipid bilayers (SLBs) have identified two general types of disruption: (1) nanoscale hole formation and (2) membrane thinning. These mechanisms have been explored using oriented circular dichroism,[22,23] X-ray diffraction,[22] solid-state NMR,[24] molecular modeling,[10,25,26] and atomic force microscopy (AFM).[10,12,23−25,27,28] The AFM/SLB assay has proven to be a particularly powerful tool for studying this problem, because it provides images of the disruption events on the nanometer scale. An interesting example of the AFM/SLB assay used MSI-78 as the nanoparticle and demonstrated that localized ∼1 nm diameter membrane thinning events occurred, as opposed to a continuous even thinning over the entire membrane.[23] In contrast, previous experiments implementing dye diffusion, enzyme leakage assays, or membrane curvature experiments were not able to provide such nanoscale mechanistic information.

We have previously shown that the degree of SLB disruption caused by polymer nanoparticles (e.g., hole formation, membrane thinning), correlates with the level of enzyme leakage, dye diffusion, cytotoxicity, and nanoparticle uptake measured in vitro (this AFM data is shown in Figures 3b−d and 4).[10,12,27] In addition, the degree of membrane disruption parallels the degree of nonselective tissue uptake

* Corresponding author. E-mail: mbanasza@umich.edu.
† Department of Chemistry, University of Michigan.
‡ Department of Physics, University of Michigan.
§ Department of Chemical Engineering, University of Michigan.
|| Michigan Nanotechology Institute for Medicine and Biological Sciences, University of Michigan.
⊥ University of Massachusetts.

10.1021/nl0722929 CCC: $40.75
Published on Web 01/25/2008

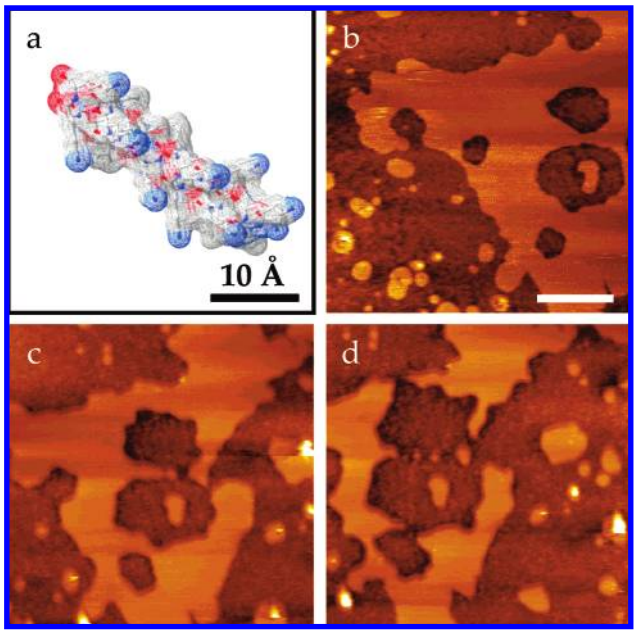

Figure 1. (a) Space-filling model of MSI-78, a 22 amino acid protein with 9 of those residues positively charged at pH 7.2. MSI-78 was injected onto a DMPC lipid bilayer (b) resulting in a final concentration of ~450 nM (1.2 mg/mL) MSI-78. Subsequent images over ~40 min were obtained (c,d), which showed the removal of lipid primarily through the expansion of pre-existing defects as is seen with G5-NH_2 dendrimers. Note that the perimeter surrounding the defect is ~1 nm thinner then the full lipid bilayer (~5 nm). This "thinning effect" is consistent with what has been previously shown at lower concentrations of MSI-78 (2 μg/mL) suggesting that the thinning of the bilayer precedes full removal of lipid. Scale bar is 500 nm.

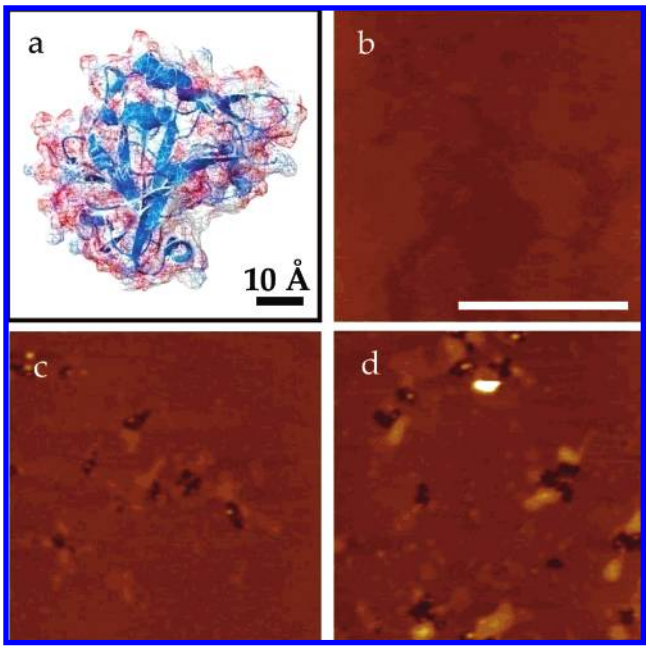

Figure 2. (a) Space-filling model of TAT, a 275 amino acid protein with 50 of those residues positively charged at pH 7.2. TAT protein was injected onto a DMPC lipid bilayer (b) yield a final concentration of ~300 nM (10 μg/mL) TAT. Subsequent images (c,d) taken over a period of ~20 min showed the formation and expansion of defects in the bilayer. Scale bar is 500 nm.

observed in vivo.[29] This correlation between the AFM/SLB assays and the in vitro and in vivo studies inspired us to examine the disruption between other nanoparticles that are well precedented to disrupt and/or translocate across cell membranes. We therefore chose the AFM/SLB assay to explore the behavior of a number of other important materials including a pentanol-core G3 PAMAM dendron, the cell penetrating peptide MSI-78,[30] the TAT sequence[31] employed by HIV virus, amine-coated gold nanoparticles,[19,32] and amine-terminated silica.[33,34] This set of particles, when combined with our previous studies on G3, G5, and G7 PAMAM dendrimers,[10] polyethyleneimine (PEI), and diethylaminoethyl-dextran (DEAE-DEX),[12] presents a wide range of physical properties (organic versus inorganic, small versus large, flexible versus rigid, spherical versus irregular) that may affect the degree of membrane disruption. This AFM/SLB assay is completed by first depositing a drop of 1 mg/mL lipid vesicle solution on a cleaved mica surface. Following an incubation time of approximately 20 min, excess lipid is removed by gently rinsing the newly formed SLB with water. After a stable image of the SLB using tapping or AC mode AFM is obtained, the nanoparticles are introduced and imaging continues until the SLB is once again stable (See Supporting Information for more experimental details).

Many biological nanomaterials found in nature are capable of traversing cell membranes. Examples include MSI-78[35] and TAT.[36] The ability to penetrate cell membranes is not only advantageous for the host and virus, respectively, but potentially also a useful tool for scientists seeking to utilize these natural transportation systems for cellular delivery. The interaction between MSI-78 and the SLB was found to be concentration-dependent. At lower concentrations (~2 μg/mL), nonuniform membrane thinning of SLBs is observed.[24] At higher MSI-78 concentrations (1.2 mg/mL), the erosion of pre-existing holes in the lipid bilayer is found (Figure 1). TAT, a larger protein in comparison to MSI-78, induces the formation of holes in the bilayer (Figure 2) at significantly lower concentrations than required for MSI-78. These SLB studies are consistent with cell level studies that have shown both of these biological proteins are internalized,[35,36] and more indirectly, are capable of disrupting cell membranes.[9−12]

A variety of polymers have been used to mimic the ability of natural particles to breach cellular membranes. PAMAM dendrimers are highly charged spherical polymers that have been employed as transfection agents in drug delivery.[2,12,37,38] Earlier studies by our group showed that the positively charged polymers interact with the supported lipid bilayer in a generation dependent fashion.[25,27] That is, G3-NH_2 dendrimers ($32e^+$) accumulate around the edges of pre-existing defects, while the more highly charged G5-NH_2 ($128e^+$) and G7-NH_2 ($512e^+$) primarily expand pre-existing defects and form new defects, respectively (Figure 3b−d). To consider a change in topology while keeping a constant chemical composition, we now present the results for pentanol-core G3-NH_2 dendrons ($16e^+$) (Figure 3a). The number of positive charges listed represent the theoretical number of amine terminal groups on each dendrimer with all amine groups expected to be protonated under the

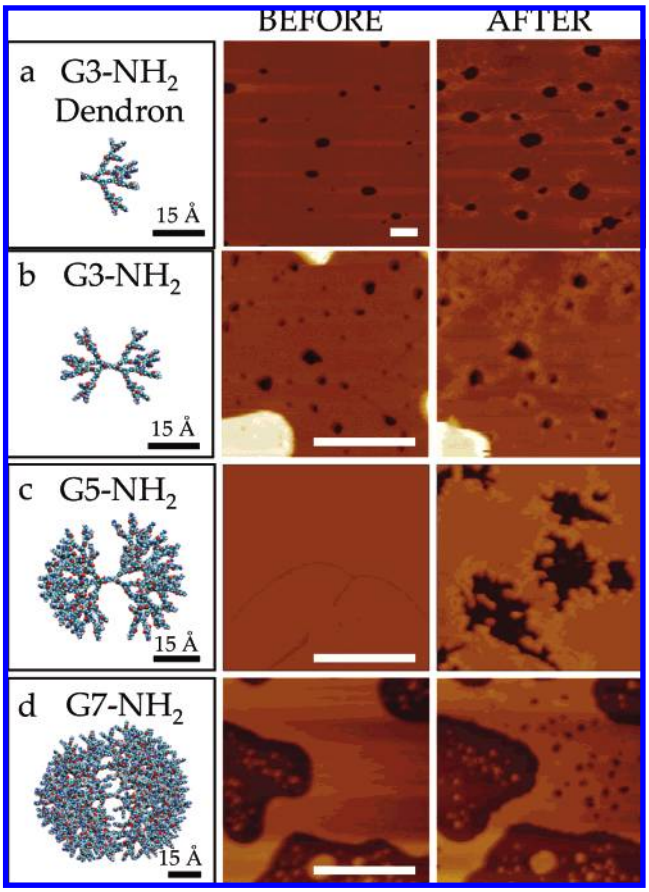

Figure 3. (a) G3-NH_2 dendron (16 e^+) primarily expanded pre-existing defects, which eventually accumulate around the edges. (b) G3-NH_2 (32 e^+) accumulated around the edges of pre-existing defects. (c) G5-NH_2 (128 e^+) primarily expanded pre-existing defects, which eventually accumulate around the edges, and (d) G7-NH_2 (512 e^+) primarily induced the formation of new defects on lipid terraces. Panel a: G3-NH_2 dendron concentration used was ~100 nM (G3-NH_2 dendron = 0.04 ug/mL). Panels b−d: dendrimer concentrations used were ~25 nM (G3-NH_2 = 0.1 ug/mL; G5-NH_2 = 0.7 ug/mL; G7-NH_2 = 3 ug/mL). Scale bars are 500 nm.

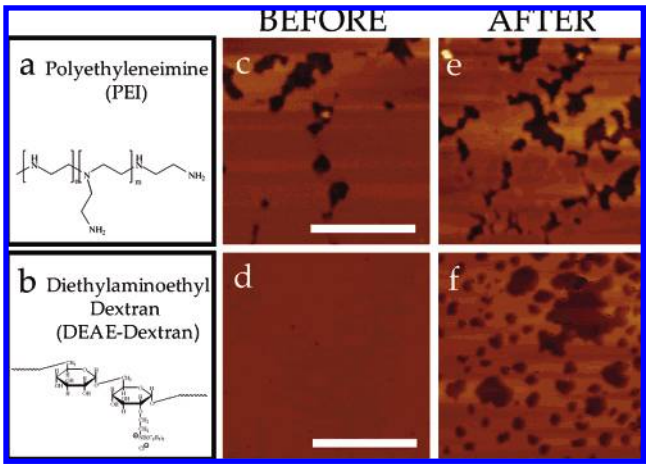

Figure 4. (a−f) PEI (M_n, 78 220; PDI, 3.44, d = 6.6 nm) and DEAE-DEX (M_n, 18 490; PDI, 32.90, d = 4.2 nm) were injected onto DMPC-supported lipid bilayers (panels a and b, respectively) yielding a final concentration of ~1 μg/mL polymer in both cases. Images following injection showed that PEI expanded pre-existing defects, panel c, similar to what is seen with G5-NH_2, while DEAE-DEX induced thinning of the bilayer similar to that seen with MSI-78 at low concentrations, panel d. Note that diameters were calculated based on M_n values and an assumed spherical shape with a density of 1.0 g/cm^3. Scale bars are 500 nm.

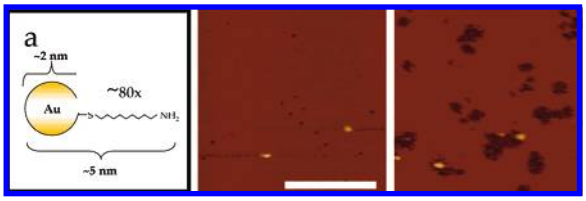

Figure 5. Au−NH_2 nanoparticles (a) were injected onto a DMPC-supported lipid bilayer (b) yielding a final concentration of ~500 nM (44 μg/mL) Au−NH_2. The Au−NH_2 nanoparticles expanded pre-existing defects within the supported lipid bilayer and appeared to aggregate on the mica surface (c). Scale bar is 500 nm.

conditions employed.[27,39] Following addition to the SLB, G3-NH_2 dendrons were shown to both accumulate around the edges of pre-existing defects, as well as expand those defects. Two commonly utilized linear polycationic polymers, PEI and DEAE-DEX, have also previously been shown to induce the formation of nanoscale defects within the model membrane (Figure 4).[12] In these cases, however, no polymer accumulation around SLB defects was witnessed.

Given the wide range of rigid nanoparticles currently in use, two inorganic nanoparticles, Au-NH_2 and silica-NH_2, were selected for testing. Gold nanoparticles are perhaps the most well studied class of nanoparticles and like dendrimers have been utilized as transfection agents.[32] The versatility of gold nanoparticles both in their tunable size and functionality make them a convenient choice in examining the effect rigidity has on nanoparticle−membrane interactions. Experiments using 2 nm gold nanoparticles coated with an alkylamine substituent (total diameter: ~5−6 nm) show that supported lipid bilayers were disrupted primarily by expanding pre-existing defects (Figure 5). This is reminiscent of what was seen in the case of G5-NH_2. Initially upon lipid erosion, the underlying mica surface is clean. However, after 6 min the Au-NH_2 nanoparticles, possibly aggregated with lipid, are observed to deposit on the negatively charged mica. PEI and PAMAM dendrimers have also been observed to bind to the mica surface.[10,12] These Au-NH_2−SLB interactions suggest that rigid-inorganic cores do not alter the gross nanoparticle−membrane interaction seen with the other classes of nanoparticles.

Although biology (in terms of proteins and receptors) and thus nanomedicine primarily focuses on the 1−15 nm scale, the 50 nm size of the silica-NH_2 particles remain pertinent given industrial uses of particles in this size range. The rigid inorganic core and amine-terminated surface of silica-NH_2 particles provide an example that is both significantly larger and does not contain a flexible, organic core or a flexible, organic surface. Despite these differences, the silica-NH_2 nanoparticles induced the formation of holes following addition to the supported lipid bilayer (Figure 6). This is similar to what was seen in the G7-NH_2 case.

Taking a broad view of these interactions, we note that the nanoparticles we studied can be divided into three

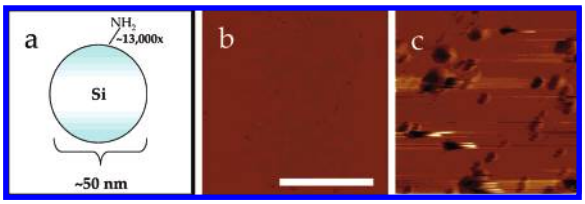

Figure 6. 50 nm amine coated silica spheres (~13,000 NH_2/sphere) (a) were introduced onto a DMPC lipid bilayer (b) yielding a final concentration ~3 mg/mL (30 nM) of the silica spheres. The addition of the positively charged spheres resulted in the formation of circular defects on the bilayer ranging from 20 to 150 nm in diameter (c). The formation of new holes within the bilayer is similar to what is seen with G7-NH_2 PAMAM dendrimers. Scale bar is 500 nm.

subcategories: (1) particles that aggregate around defects and on the lipid bilayer surface (PAMAM G3-NH_2) but are not effective at inducing defects, (2) particles that encounter the surface, do not directly induce defects, but instead diffuse to existing defects and expand them (Au-NH_2, MSI-78, pentanol-core G3-NH_2 dendron, PAMAM G5-NH_2), and (3) particles that are capable of directly inducing defects in lipid bilayers (TAT, PAMAM G7-NH_2, PEI, DEAE-DEX and silica-NH_2). On the basis of these studies, cationic nanoparticles with quite different sizes, shapes, and flexibility are all capable of disrupting SLBs.

When making qualitative comparisons between these particles, one must recall that the concentrations used for the imaging experiments differ. In all cases, the images are showing the concentration range where the particles disrupt the bilayer. Keeping this in mind, we note that cationic charge density does not serve as a good predictor of the interaction across nanoparticle classes. However, over the size ranges studied, the surface area of cationic nanoparticles does roughly correlate with the degree of nanoparticle−lipid disruption. Those particles that have greater surface areas ($>\sim$60 nm^2) are generally more effective at inducing SLB disruption than those with smaller surface area ($<\sim$60 nm^2). These smaller nanoparticles are more likely to aggregate on the surface around pre-existing defects.

The results presented within this paper are consistent with several studies previously performed by other groups. A thermodynamic model describing the mechanism of interaction between PAMAM dendrimers, and more generally nanoparticles, and lipid bilayers has recently been completed by Ginzburg and Balijepalli.[40] They demonstrated that charged nanoparticles with diameters comparable to that of a lipid bilayer show an increased tendency to induce defect formation within lipid bilayers. Our results, as well as those of Ginzburg and Balijepalli, are also consistent with the observations of Oberdorster et al. who demonstrated that ultrafine particles (diameter ~20 nm) induce an increased inflammatory response over "fine particles" (diameter ~250 nm) per unit mass.[41,42] Here, Oberdorster et al. attributed the origin of this difference to the larger ratio of surface to mass inherently present in ultrafine particles over fine particles.[41] Note that in the work of Oberdorster et al. surface area was defined per mass of sample, whereas for the work presented in this paper surface area is defined per particle. This difference in the definition of particle characteristics results in Oberdorster et al. concluding that for a given mass of sample that the smaller particles will be more disruptive. In this paper, surface area is defined per particle, resulting in the conclusion that for a given number of nanoparticles, the larger particles (which have greater surface area) are more disruptive. Although surface area is a general parameter for predicting how cationic nanoparticles interact with SLBs, the trends presented here indicate that it is not the only important parameter. The nanoparticle−SLB interactions are likely also dependent on a number of other parameters including charge density, shape, flexibility, and amphipathic character.

These results presented in this paper demonstrate that disruption of lipid bilayers is a common property of cationic nanoparticles. Each cationic nanoparticle presented here, regardless of shape (spherical versus irregular), chemical composition (organic versus inorganic), deformability (flexible versus rigid), charge density, or size, disrupts supported lipid bilayers. Our previously published studies demonstrated that effectiveness of a particle in causing nanoscale disruption of supported lipid bilayers correlated well with the particle's ability to both induce cell membrane permeability and to internalize into the cell.[10,12,13] The data presented here indicates that the hypothesis that nanoscale hole formation may be a biologically relevant process should be extended to a variety of additional materials including MSI-78, TAT, and cationic gold and silica particles. The generality of the bilayer disruption is extremely important because many examples of natural and synthetic nanoparticles utilize amine terminations to achieve water solubility and other functions. Given the growing use of nanoparticles in consumer products, industrial applications, and in medicine, it is imperative that we understand observed and potential effects of nanoparticles on biological membranes and the basic science underpinning these interactions.

Acknowledgment. We would like to acknowledge the National Institutes of Health for funding this research under National Institute of Biomedical Imaging and Engineering Grant EB005028 (M.M.B.H.) and National Institute of General Medical Sciences Grant GM077173 (V.R.).

Supporting Information Available: Experimental details. This material is available free of charge via the Internet at http://pubs.acs.org.

References

(1) Popielarski, S. R.; Pun, S. H.; Davis, M. E. *Bioconjugate Chem.* **2005**, *16* (5), 1063−1070.
(2) Bielinska, A. U.; Yen, A.; Wu, H. L.; Zahos, K. M.; Sun, R.; Weiner, N. D.; Baker, J. R.; Roessler, B. J. *Biomaterials* **2000**, *21* (9), 877−887.
(3) Bell, A. T. *Science* **2003**, *299* (5613), 1688−1691.
(4) Allen, N. S.; Edge, M.; Ortega, A.; Liauw, C. M.; Stratton, J.; McIntyre, R. B. *Polym. Degrad. Stab.* **2002**, *78* (3), 467−478.
(5) Luppi, B.; Cerchiara, T.; Bigucci, F.; Basile, R.; Zecchi, V. *J. Pharm. Pharmacol.* **2004**, *56* (3), 407−411.
(6) Maynard, A. D.; Kuempel, E. D. *J. Nanopart. Res.* **2005**, *7* (6), 587−614.
(7) Magrez, A.; Kasas, S.; Salicio, V.; Pasquier, N.; Seo, J. W.; Celio, M.; Catsicas, S.; Schwaller, B.; Forro, L. *Nano Lett.* **2006**, *6* (6), 1121−1125.

(8) Xia, T.; Kovochich, M.; Brant, J.; Hotze, M.; Sempf, J.; Oberley, T.; Sioutas, C.; Yeh, J. I.; Wiesner, M. R.; Nel, A. E. *Nano Lett.* **2006**, *6* (8), 1794−1807.
(9) Fischer, D.; Li, Y. X.; Ahlemeyer, B.; Krieglstein, J.; Kissel, T. *Biomaterials* **2003**, *24* (7), 1121−1131.
(10) Hong, S. P.; Bielinska, A. U.; Mecke, A.; Keszler, B.; Beals, J. L.; Shi, X. Y.; Balogh, L.; Orr, B. G.; Baker, J. R.; Holl, M. M. B. *Bioconjugate Chem.* **2004**, *15* (4), 774−782.
(11) Hussain, S. M.; Hess, K. L.; Gearhart, J. M.; Geiss, K. T.; Schlager, J. J. *Toxicol. in Vitro* **2005**, *19* (7), 975−983.
(12) Hong, S. P.; Leroueil, P. R.; Janus, E. K.; Peters, J. L.; Kober, M. M.; Islam, M. T.; Orr, B. G.; Baker, J. R.; Holl, M. M. B. *Bioconjugate Chem.* **2006**, *17* (3), 728−734.
(13) Leroueil, P. R.; Hong, S. Y.; Mecke, A.; Baker, J. R.; Orr, B. G.; Holl, M. M. B. *Acc. Chem. Res.* **2007**, *40* (5), 335−342.
(14) Monteiro-Riviere, N. A.; Nemanich, R. J.; Inman, A. O.; Wang, Y. Y. Y.; Riviere, J. E. *Toxicol. Lett.* **2005**, *155* (3), 377−384.
(15) Oberdorster, E. *Environ. Health Perspect.* **2004**, *112* (10), 1058−1062.
(16) Oberdorster, E.; Cheek, A. O. *Environ. Toxicol. Chem.* **2001**, *20* (1), 23−36.
(17) Oberdorster, G.; Gelein, R. M.; Ferin, J.; Weiss, B. *Inhalation Toxicol.* **1995**, *7* (1), 111−124.
(18) Tinkle, S. S.; Antonini, J. M.; Rich, B. A.; Roberts, J. R.; Salmen, R.; DePree, K.; Adkins, E. J. *Environ. Health Perspect.* **2003**, *111* (9), 1202−1208.
(19) Goodman, C. M.; McCusker, C. D.; Yilmaz, T.; Rotello, V. M. *Bioconjugate Chem.* **2004**, *15* (4), 897−900.
(20) Ottaviani, M. F.; Sacchi, B.; Turro, N. J.; Chen, W.; Jockusch, S.; Tomalia, D. A. *Macromolecules* **1999**, *32* (7), 2275−2282.
(21) Kapoor, S.; Kartha, S.; Meisel, D. *Res. Chem. Intermed.* **2001**, *27* (4−5), 317−332.
(22) Heller, W. T.; Waring, A. J.; Lehrer, R. I.; Harroun, T. A.; Weiss, T. M.; Yang, L.; Huang, H. W. *Biochemistry* **2000**, *39* (1), 139−145.
(23) Mecke, A.; Lee, D. K.; Ramamoorthy, A.; Orr, B. G.; Holl, M. M. B. *Langmuir* **2005**, *21* (19), 8588−8590.
(24) Mecke, A.; Lee, D. K.; Ramamoorthy, A.; Orr, B. G.; Holl, M. M. B. *Biophys. J.* **2005**, *89* (6), 4043−4050.
(25) Mecke, A.; Uppuluri, S.; Sassanella, T. M.; Lee, D. K.; Ramamoorthy, A.; Baker, J. R.; Orr, B. G.; Holl, M. M. B. *Chem. Phys. Lipids* **2004**, *132* (1), 3−14.
(26) Livadaru, L.; Kovaenko, A. *Nano Lett.* **2006**, *6* (1), 78−83.
(27) Mecke, A.; Majoros, I. J.; Patri, A. K.; Baker, J. R.; Holl, M. M. B.; Orr, B. G. *Langmuir* **2005**, *21* (23), 10348−10354.
(28) Spurlin, T. A.; Gewirth, A. A. *Biophys. J.* **2006**, *91* (8), 2919−2927.
(29) Nigavekar, S. S.; Sung, L. Y.; Llanes, M.; El-Jawahri, A.; Lawrence, T. S.; Becker, C. W.; Balogh, L.; Khan, M. K. *Pharm. Res.* **2004**, *21* (3), 476−483.
(30) Drin, G.; Cottin, S.; Blanc, E.; Rees, A. R.; Temsamani, J. *J. Biol. Chem.* **2003**, *278* (33), 31192−31201.
(31) Richard, J. P.; Melikov, K.; Vives, E.; Ramos, C.; Verbeure, B.; Gait, M. J.; Chernomordik, L. V.; Lebleu, B. *J. Biol. Chem.* **2003**, *278* (1), 585−590.
(32) Sandhu, K. K.; McIntosh, C. M.; Simard, J. M.; Smith, S. W.; Rotello, V. M. *Bioconjugate Chem.* **2002**, *13* (1), 3−6.
(33) Mori, H.; Lanzendorfer, M. G.; Muller, A. H. E.; Klee, J. E. *Langmuir* **2004**, *20* (5), 1934−1944.
(34) Bagwe, R. P.; Hilliard, L. R.; Tan, W. H. *Langmuir* **2006**, *22* (9), 4357−4362.
(35) Fuchs, P. C.; Barry, A. L.; Brown, S. D. *Antimicrob. Agents Chemother.* **1998**, *42* (5), 1213−1216.
(36) Fawell, S.; Seery, J.; Daikh, Y.; Moore, C.; Chen, L. L.; Pepinsky, B.; Barsoum, J. *Proc. Natl. Acad. Sci. U.S.A.* **1994**, *91* (2), 664−668.
(37) Shukla, R.; Thomas, T. P.; Peters, J. L.; Desai, A. M.; Kukowska-Latallo, J.; Patri, A. K.; Kotlyar, A.; Baker, J. R. *Bioconjugate Chem.* **2006**, *17* (5), 1109−1115.
(38) Thomas, T. P.; Patri, A. K.; Myc, A.; Myaing, M. T.; Ye, J. Y.; Norris, T. B.; Baker, J. R. *Biomacromolecules* **2004**, *5* (6), 2269−2274.
(39) Majoros, I. J.; Myc, A.; Thomas, T.; Mehta, C. B.; Baker, J. R. *Biomacromolecules* **2006**, *7* (2), 572−579.
(40) Ginzburg, V. V.; Balijepalli, S. *Nano Lett.* **2007**, *7*, 3716−3722.
(41) Oberdorster, G. *Int. Arch. Occup. Environ. Health* **2001**, *74* (1), 1−8.
(42) Oberdorster, G.; Oberdorster, E.; Oberdorster, J. *Environ. Health Perspect.* **2005**, *113* (7), 823−839.

NL0722929